

# Antisense-induced Myostatin Exon Skipping Leads to Muscle Hypertrophy in Mice Following Octa-guanidine Morpholino Oligomer Treatment

Jagjeet K Kang<sup>1</sup>, Alberto Malerba<sup>1</sup>, Linda Popplewell<sup>1</sup>, Keith Foster<sup>1</sup> and George Dickson<sup>1</sup>

<sup>1</sup>School of Biological Sciences, Royal Holloway—University of London, Surrey, UK

Myostatin is a negative regulator of muscle mass, and several strategies are being developed to knockdown its expression to improve muscle-wasting conditions. Strategies using antimyostatin-blocking antibodies, inhibitory-binding partners, signal transduction blockers, and RNA interference system (RNAi)-based knockdown have yielded promising results and increased muscle mass in experimental animals. These approaches have, however, a number of disadvantages such as transient effects or adverse immune complications. We report here the use of antisense oligonucleotides (AOs) to manipulate myostatin pre-mRNA splicing and knockdown myostatin expression. Both 2′O-methyl phosphorothioate RNA (2′OMePS) and phosphorodiamidate morpholino oligomers (PMO) led to efficient exon skipping *in vitro* and *in vivo* and knockdown of myostatin at the transcript level. The substantial myostatin exon skipping observed after systemic injection of Vivo-PMO into normal mice led to a significant increase in soleus muscle mass as compared to the controls injected with normal saline suggesting that this approach could be feasible to ameliorate muscle-wasting pathologies.

Received 8 June 2010; accepted 4 September 2010; published online 5 October 2010. doi:10.1038/mt.2010.212

## INTRODUCTION

A range of strategies have been proposed to enhance muscle bulk and strength as a treatment for a number of age-related muscle disorders and various neuromuscular disorders, including muscular dystrophies. Myostatin, a transforming growth factor- $\beta$  family member, also called growth and differentiation factor-8, is a negative regulator of muscle growth and the myostatin signaling axis has been a major focus in such strategies. Myostatin null or hypomorphic animals are significantly larger than wild-type animals and show a large increase in skeletal muscle mass.<sup>1</sup> The first natural myostatin mutation in humans has also been identified in a young boy.<sup>2</sup> Myostatin blockade, therefore, offers a strategy for counteracting muscle-wasting conditions including Duchenne muscular dystrophy.<sup>3</sup> Delivery

of myostatin-inhibiting genes, including growth and differentiation factor-associated serum protein-1 (*GASP-1*), follistatin-related gene (*FLRG*), follistatin-344 (*FS*) and myostatin propeptide, via adeno-associated virus,<sup>4–6</sup> lead to an increase in muscle mass in treated animals, with the greatest increase in FS-treated animals.<sup>7</sup> Use of potentially therapeutic antimyostatin-blocking antibodies of high-binding affinity has proved to be a promising strategy. However, there are some constraints related to the use of antimyostatin antibodies that include difficulty in long-term sustainability, undesirable immune responses, and inhibitory effects not precisely specific to myostatin in regard to muscle growth.<sup>8,9</sup> Significant increase in skeletal muscle mass was also observed using adeno-associated virus vectors to deliver a recombinant myostatin propeptide gene fragment, or by a retrovirus-based RNA interference system (RNAi).<sup>4,6,10</sup> Both approaches have safety concerns of possible genotoxicity, due to uncontrolled vector genome insertion into host chromosomes.<sup>11</sup> The RNAi system faces an additional hurdle in terms of effective delivery of the RNAi molecules into the disease models for clinical studies.<sup>12</sup> RNA-based modulation therapy has the potential to overcome difficulties encountered by conventional gene therapy methods. Antisense oligonucleotides (AOs) are capable of hybridizing to a sense target sequence leading to cleavage of the RNA:DNA hybrid by RNase H which results in downregulation of gene transcription.<sup>13,14</sup> In an alternative approach, antisense-mediated modulation of pre-mRNA splicing has been pioneered by Dominski and Kole.<sup>15</sup> In the first experiments, AOs were aimed at activated cryptic splice sites in the  $\beta$ -globin (*HBB*) and cystic fibrosis transmembrane conductance regulator (*CFTR*) genes in order to restore normal splicing in  $\beta$ -thalassemia and cystic fibrosis patients.<sup>15–17</sup> The identification of exon/intron boundaries by the splicing machinery, and therefore inclusion of the exons into the mRNA, is extensively thought to depend on exonic splicing enhancer (ESE) motifs.<sup>18</sup> By masking these ESE sites with sequence-optimized AOs, the targeted exons are no longer recognized as exons, and are spliced out with neighboring introns. This so-called antisense-induced exon skipping has already been used clinically to partly correct the mutated dystrophin and convert the severe Duchenne muscular dystrophy phenotype into a milder Becker muscular dystrophy phenotype.<sup>19</sup>

The first two authors contributed equally to this work.

Correspondence: George Dickson, School of Biological Sciences, Royal Holloway—University of London, Egham, Surrey TW20 0EX, UK.  
E-mail: G.Dickson@rhul.ac.uk

Clinical trials to determine the safety profile and the efficacy of single intramuscular doses of two different chemistries of AOs, 2'-O-methyl phosphorothioate (2'OMePS) AOs and phosphorodiamidate morpholino oligomers (PMOs) in Duchenne muscular dystrophy patients have recently been completed.<sup>20,21</sup> The treatments were well tolerated by all the patients and the injection of AOs induced the production of dystrophin. 2'OMePS AOs, being negatively charged, are easily delivered *in vitro*, whereas PMOs are capable of more sustained effect *in vivo* due to their resistance to enzymatic degradation<sup>22</sup> and owing to their longer sequence, have increased affinity to target.<sup>23</sup> When conjugated with various peptide derivatives, or with dendrimeric octa-guanidine (so-called Vivo-morpholino), PMOs demonstrate a significantly increased delivery in the case of dystrophin skipping.<sup>24,25</sup> We have adopted this approach of using AOs with different chemistries, so enhancing their half-lives relative to the RNAi molecules, to investigate the outcome of myostatin knockdown by exon skipping. Skipping of exon 2 (374 nucleotides) of myostatin is predicted to lead to an out-of-phase splicing of exons 1 and 3, and knockdown of myostatin due to truncation of the Open Reading Frame and nonsense-mediated mRNA decay. The data we present here constitute a proof-of-principle that oligonucleotide-mediated antisense exon skipping leads to a physiologically significant myostatin knockdown *in vitro* and *in vivo*. This type of antisense treatment could thus

potentially form part of an effective strategy to improve various muscle-wasting conditions, and along with dystrophin rescue or augmentation, to treat Duchenne muscular dystrophy.

## RESULTS

### Bioinformatics analysis and design of specific AOs predicted to induce skipping of myostatin exon 2

Bioinformatics analysis of exon 2 of myostatin was performed using three bioinformatics tools, ESE finder,<sup>26,27</sup> PESX,<sup>28,29</sup> and Rescue ESE,<sup>30</sup> to identify and locate ESEs and exonic splicing suppressor or silencer motifs. The output of these algorithms is displayed in **Figure 1a**. A series of overlapping AOs were designed and synthesized as 2'OMePSs and PMOs to span sequences where clusters of ESEs which were predicted by one or more of the programs coincide. The sequences of the AOs are available on request.

### High levels of myostatin exon 2 skipping in C2C12 cell culture following treatment with a range of AOs

In order to verify the efficiency of these AO target sequences, C2C12 muscle cell cultures were transfected with the 2'OMePS oligomers, and nested reverse transcriptase-PCR (RT-PCR) for skipping of myostatin performed on the RNA extracted from transfected and control cells. A representative horizontal agarose gel electrophoresis separation of products obtained is shown in **Figure 1b**. The level of skipping produced by each AO at 250 nmol/l

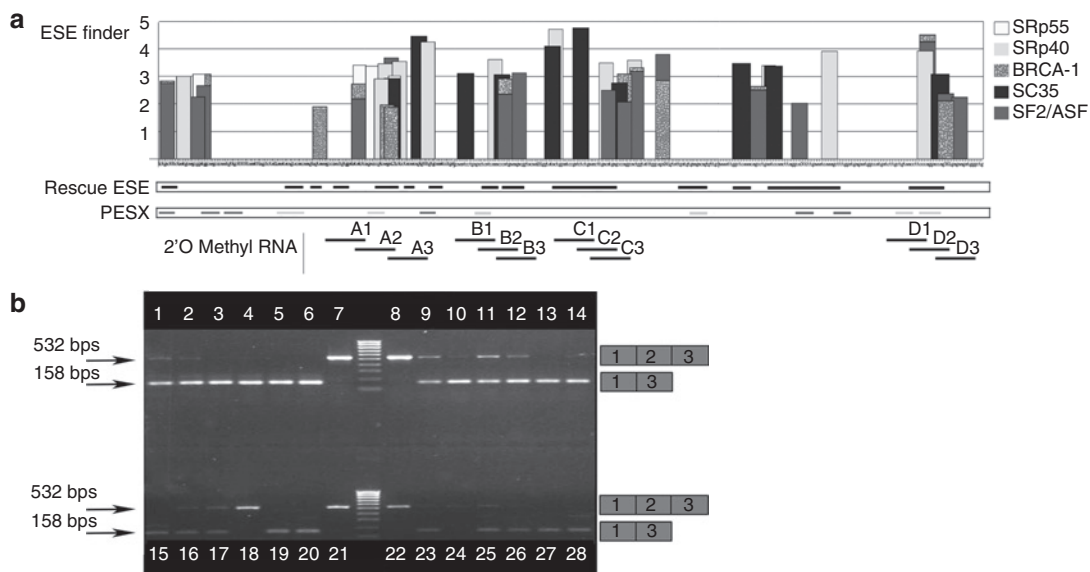


**Figure 1** Bioinformatics analysis, design, and evaluation in C2C12 muscle cells of specific AOs predicted to induce skipping of myostatin exon 2. **(a)** Results from three algorithms used to identify ESE sequences for designing of exon skipping AOs targeting exon 2 of the mouse myostatin gene. The ESE Finder analysis shows the location and values above threshold for SR protein-binding motifs, SF2/ASF, SF2/ASF (BRCA 1), SC35, SRp40, and SRp55 which are shown as vertical bars above the sequence of exon 2. The Rescue ESE analysis shows the position of possible exonic splicing enhancer sites by black horizontal lines parallel to the sequence of exon 2. The PESX analysis shows the location of ESEs as light gray horizontal lines, and exon splicing silencers (ESSs) as dark gray horizontal lines. The bold horizontal ladder black lines represent the sequence of the 20-mer 2'OMePSs which were obtained after aligning the outputs from the three algorithms. **(b)** Comparison of efficacy of different 2'OMePS oligomers to induce skipping of exon 2 in myostatin mRNA from C2C12 cell cultures. RT-PCR was performed on 1 µg mRNA from C2C12 cells treated with 12 different 2'OMePS oligomers at 250 nmol/l. Transfections were performed in duplicates and the nested RT-PCR products were loaded on 1.2% agarose gel as follow: Tracks 1 and 2: oligomer A1; Tracks 3 and 4: oligomer A2; Tracks 5 and 6: oligomer A3; Tracks 9 and 10: oligomer B1; Tracks 11 and 12: oligomer B2; Tracks 13 and 14: oligomer B3; Tracks 15 and 16: oligomer C1; Tracks 17 and 18: oligomer C2; Tracks 19 and 20: oligomer C3; Tracks 23 and 24: oligomer D1; Tracks 25 and 26: oligomer D2; Tracks 27 and 28: oligomer D3; Tracks 7, 8, 21 and 22: controls with transfection reagent Lipofectamine 2000 alone, but no AO; Size Marker used is Hyper ladder IV. 2'OMePS, 2'-O-methyl phosphorothioate RNA; AO, antisense oligonucleotide; bp, base pairs; ESE, exonic splicing enhancer; RT-PCR, reverse transcriptase-PCR.

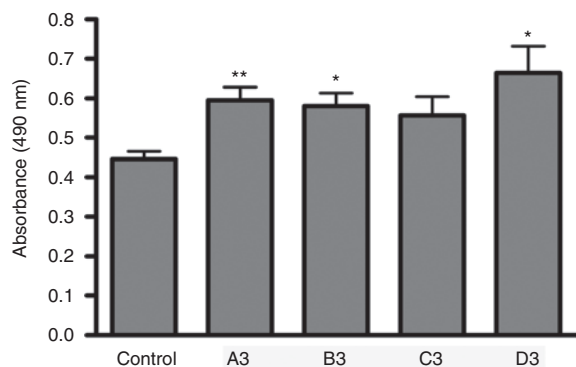


**Figure 2** Antisense-induced myostatin exon 2 skipping with 2'OMePS oligomers leads to an increase in C2C12 cell proliferation. C2C12 cells were treated with a range of 2'OMePS oligomers along with lipofectamine 2000 (LF2000), and assayed 24 hours later for cell proliferation by lactic dehydrogenase assay. Treatment with 2'OMePS oligomers A3, B3, and D3 resulted in significant increases in the number of cells after 24 hours compared to the cultures treated with only transfection reagent LF2000 but no AO. C3 did not induce a substantial change. (*t*-test analysis, *n* = 6; \**P* < 0.05; \*\**P* < 0.01). 2'OMePS, 2'-O-methyl phosphorothioate RNA.

was determined semiquantitatively using densitometric analysis.<sup>31</sup> All of the designed 2'OMePSs were observed to induce myostatin exon 2 skipping in C2C12 cultures but at various levels of relative efficiency. A2 and A3 induced almost 100% skipping; B3 (74%), C3 (41%), and D3 (48%) also induced a considerable level of skipping. The nature of putative antisense-induced PCR exon1–exon3 splicing product was confirmed by sequencing the products (data not shown).

### Antisense-induced myostatin exon 2 skipping and myostatin knockdown leads to an increase in C2C12 cell proliferation

In order to verify that AO-mediated myostatin exon 2 skipping and knockdown, lead to a significant biological response, the autocrine activity of myostatin on C2C12 cell proliferation was evaluated following treatment of cultures with 2'OMePSs targeting myostatin exon 2. The cell proliferation assay was based on determination of lactic dehydrogenase activity of metabolically active cells. The results of the proliferation assay clearly showed a remarkable difference in cell proliferation in C2C12 cells treated with myostatin exon 2 AOs compared to mock-transfected control cells (Figure 2). Statistical analysis of the data using individual paired *t*-tests showed that oligomers A3 (*P* = 0.0031), B3 (*P* = 0.0055) and D3 (*P* = 0.0115) induced a significant increase in cell proliferation, as compared to mock transfected control cells. Oligomer C3 (*P* = 0.0534) did not produce a statistically significant change.

### Demonstration of exon skipping in mouse following intramuscular injection of 2'OMePS oligomers targeting myostatin exon 2

On the basis of RT-PCR results obtained from the *in-vitro* studies, two 2'OMePS oligomers (A2 and B3) were selected to evaluate their ability to induce efficient exon skipping *in vivo*. The 2'OMePS oligomers (3 nmol) were administered by intramuscular injection into tibialis anterior (TA) muscles of mice. Two and

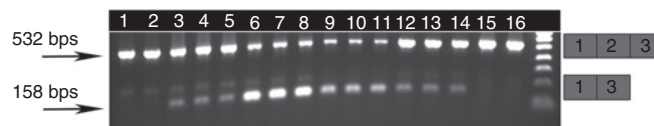


**Figure 3** Exon skipping in mouse following intramuscular injection of 2'OMePS oligomers targeting myostatin exon 2. Oligomers A2 and B3 (3 nmol) were administered by a single intramuscular injection into the tibialis anterior (TA) muscles of mice. Two and four weeks later, muscles were recovered, and RNA extracted and analyzed for the presence of myostatin exon 2 skipping by RT-PCR. Agarose ethidium bromide gel electrophoresis is shown for the products of RT-PCR analysis: The upper and lower bands correspond to the normal exon 1, 2, and 3 product (532 bp) and the exon 2 skipped product (158 bp), respectively which were verified by sequencing (data not shown). The faint shadow band of intermediate migration in some tracks was found upon sequencing to correspond to a product containing a partial sequence of exon 2 due to a cryptic 3' splice site 296 nt downstream of the correct one. Tracks 1 and 2: 14 days control; Tracks 3–5: 14 days A2-treated; Tracks 6–8: 28 days A2-treated; Tracks 9–11: 14 days B3-treated; Tracks 12–14: 28 days B3-treated; Tracks 15 and 16: 28 days control. Densitometric evaluation of the skipped and unskipped bands showed that after 14 days, A2 gave 25.6% and B3 54.6% skipping, and after 28 days, A2 gave 48.6% and B3 24.5% skipping. 2'OMePS, 2'-O-methyl phosphorothioate RNA; bps, base pairs; nt, nucleotides; RT-PCR, reverse transcriptase-PCR.

four weeks after the injections, muscles were recovered, weighed, RNA extracted and analyzed for the presence of myostatin exon 2 skipping by RT-PCR. Both reagents (A2 and B3) induced significant level of myostatin exon 2 skipping at either the 2 weeks and 4 weeks time points after a single 2'OMePS oligomer administration (Figure 3). Densitometric quantification of full-length and skipped product bands from the RT-PCR analyses of RNA was performed to detect which of the two 2'OMePSs tested was the more efficient *in vivo*. Oligomer A2 gave 25.6% skipping, and B3 gave 54.6% skipping at the 2 weeks time point. However, after 4 weeks, A2 gave 48.6% skipping whereas B3 gave 24.5% skipping. Although the skipping of myostatin exon 2 was evident, the effect was not sufficient to see a significant change in TA muscle mass (data not shown). From previous work on exon skipping for dystrophin, it is well established that the intramuscular injections of naked unconjugated AOs in undamaged muscles are not very efficient.<sup>25</sup>

### High levels of myostatin exon 2 skipping in C2C12 cell culture following treatment with a range of PMOs designed on the basis of 2'OMePS data

The animal studies above established that exon skipping of the myostatin gene observed after intramuscular injection of 2'OMePS AOs was insufficient to induce change in TA mass. The PMO chemistry has been demonstrated to have very high efficiency *in vivo*.<sup>32</sup> Therefore, PMOs were designed on the basis of most efficient 2'OMePS AOs (A3, B3, C3, and D3) and initially tested *in vitro*. PMOs are uncharged chemicals and do not directly interact with the polycationic transfection reagent lipofectamine 2000. In order to enable reasonable transfection efficiency in C2C12 cells, PMOs were hybridized to complementary so-called leash oligonucleotides of natural negatively charged DNA chemistry as previously described.<sup>23,33,34</sup> Nested RT-PCR analysis of mRNA harvested from C2C12 cells treated with leashed-PMO lipoplexes demonstrated that exon skipping was induced by all the PMOs



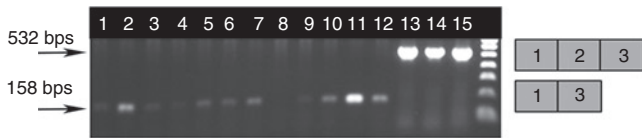


**Figure 4** Myostatin exon 2 skipping in C2C12 cell culture following treatment with a range of leashed-PMO lipoplexes. C2C12 cell cultures treated with a range of leashed-PMOs in lipoplex form with LF2000 exhibited skipping of exon 2 in myostatin mRNA. RT-PCR was performed on 1  $\mu$ g mRNA from C2C12 cells treated with 250nmol/l PMOs (designed on the basis of the most effective 2'OMePS sequences: A3, B3, C3, and D3) over a period of 24 hours. Transfections were performed in triplicate and RT-PCR products were loaded on 1.2% agarose gel as follows: Tracks 1–3: PMO-A; Tracks 4–6: PMO-B; Tracks 7–9: PMO C; Tracks 10–12: PMO-D; Tracks 13–15: LF2000-treated control; bps, base pairs; LP2000, lipofectamine 2000; PMO, phosphorodiamidate morpholino oligomers; RT-PCR, reverse transcriptase-PCR.

tested (**Figure 4**). Sequencing of the PCR products verified accurate skipping of the targeted exon by both AO chemistries tested here (data not shown).

### Systemic injection of PMOs conjugated to octa-guanidine dendrimer resulted in myostatin exon skipping associated with a significant increase in muscle mass and myofiber size

The conjugation of PMO with octa-guanidine dendrimer (so-called Vivo-PMOs) significantly increases the delivery and efficiency of PMO directed against exon 23 of dystrophin compared to unmodified PMO.<sup>25</sup> Therefore, a Vivo-PMO based on the sequence of the previously tested 2'OMePS oligomer, D3, was produced to evaluate systemic intravascular treatment regimes. Mice were treated with 6 mg/kg of Vivo-PMO-D3 by five weekly intravenous injections, and whole body weight and the mass of TA, soleus, and extensor digitorum longus (EDL) muscles were recorded 10 days after the last injection. Among the muscles analyzed in the treated animals the soleus showed a statistically significant change in mass ( $P = 0.034$ ) (**Figure 5a**). In accordance with this, high levels of exon skipping of myostatin exon 2 was demonstrated at the transcript level in soleus (79%), whereas a very low level of skipping was observed in EDL muscle (9%) (**Figure 5b**). Importantly, the cross-sectional area (CSA) of soleus muscle fibers in treated animals significantly increased ( $P < 0.0001$ ; mean CSA were  $254 \pm 5 \mu\text{m}^2$  for control and  $333 \pm 3 \mu\text{m}^2$  for PMO-treated animals ( $n = 6$ ) with a significant shift on the distribution of CSA ( $\chi^2 = 38.34$ ;  $df = 12$ ) (**Figure 5c, d**). No change was observed in the CSA of EDL muscle (data not shown).

### DISCUSSION

It has been well established that myostatin is a negative regulator of skeletal muscle mass<sup>35</sup> and several approaches have been used to knockdown this factor to induce an increase in skeletal muscle growth.<sup>36</sup> The use of AOs to induce exon skipping and thereby knockdown the expression of myostatin presents several advantages over the other currently used gene therapy approaches. Firstly, there is no risk of uncontrolled insertion into the genome with AOs as in case of virus-mediated approaches.<sup>37</sup> Moreover, with an appropriate dosing regimen, exon skipping levels can be regulated and, if necessary the treatment can be interrupted. Importantly AOs have

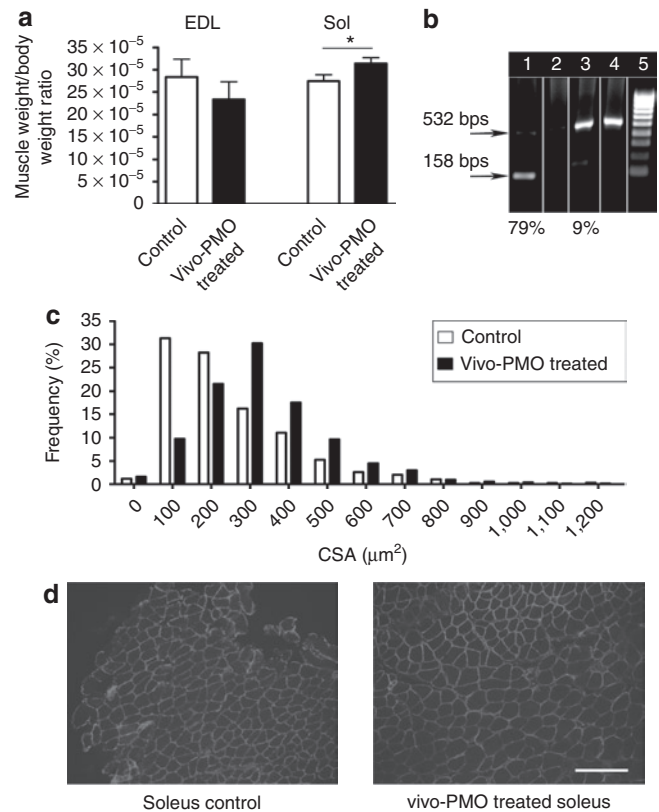


**Figure 5** Systemic injection of PMO conjugated to octa-guanidine dendrimer (Vivo-PMO) results in myostatin exon skipping associated with a significant increase in muscle mass and myofiber size. Mice were treated with 6 mg/kg of Vivo-PMO-D3 by five weekly intravenous injections, and muscles harvested for RNA extraction and immunohistology 10 days later. **(a)** Weight of soleus and EDL muscle after treatment. Weights of soleus muscles were significantly increased ( $t$ -test,  $P < 0.034$ ;  $n = 6$ ) whereas weights of EDL muscles showed no significant change. **(b)** RT-PCR was carried out on 1  $\mu$ g RNA from soleus and EDL muscles and products resolved on a 1.2% agarose gel. Track 1: Vivo-PMO treated soleus; Track 2: control soleus; Track 3: Vivo-PMO treated EDL; Track 4: control EDL. **(c)** Distribution of myofiber sizes (CSA) in vivo-PMO treated (black bars) and control (open bars) soleus muscles. **(d)** Representative dystrophin immunohistology indicating increased myofiber CSA in vivo-PMO treated compared to control soleus muscle cryosections. Bar = 500  $\mu\text{m}$ . CSA, cross-sectional area; EDL, extensor digitorum longus; PMO, phosphorodiamidate morpholino oligomers; RT-PCR, reverse transcriptase-PCR.

not been reported to produce any toxic effects or immune response so far in animal models as well as when used in clinical application.<sup>38</sup> Here, we show that AOs of 2'OMePS chemistry, designed using bioinformatics algorithms, resulted in a substantial level of myostatin exon 2 skipping *in vitro*. Myostatin being an inhibitor of myogenic differentiation, controls the proliferation of myoblasts.<sup>39</sup> Therefore, myostatin knockdown is expected to increase the cell proliferation. The AOs designed were biologically active and induced an increase in C2C12 cell proliferation. The efficacy of knockdown by exon skipping *in vivo* has proved to be more challenging to establish than *in vitro*. The efficiency of myostatin skipping was verified by injecting 2'OMePS intramuscularly. The intramuscular treatment of a single muscle induced exon skipping, but did not appear to affect myostatin activity. This is likely to be due to supply of biologically active myostatin to the injected

muscle by the bloodstream. Moreover, in a hypothetical clinical approach, the whole body should be treated. For these reasons, we decided to administer the AOs by systemic tail vein injection in our further experiments. PMO chemistry was chosen for this experiment due to its better stability compared to the 2'OMePS and also because PMOs have been reported to have a longer effect *in vivo*.<sup>40</sup> This is particularly important for knocking down proteins like myostatin, which do not have a long half-life like dystrophin. The PMO sequence used for the systemic administration study induced efficient skipping *in vitro*. It also maps in a region totally conserved between mouse and human myostatin paving the way to test the same PMO for clinical applications in humans. In order to achieve a reasonable effect in undamaged muscles, a PMO conjugated to a delivery moiety has to be used.<sup>41</sup> Vivo-PMO is commercially available and has been reported to be effective in normal healthy mice.<sup>25</sup> By injecting Vivo-PMO, a substantial increase in muscle size and the change of CSA fiber distribution has been obtained, but only in the soleus muscle. The differential response in EDL and soleus may be due in part to a greater amount of ActRIIb being expressed on the surface of EDL muscle, or because the intrinsic level of myostatin is greater in fast (myosin type IIb positive) myofibres.<sup>46</sup> Alternatively, we can speculate that the dosing regimen used, which has been reported to be optimal for Vivo-PMO for exon skipping of dystrophin gene,<sup>25</sup> does not achieve sufficient skipping of myostatin gene in EDL. In the case of dystrophin skipping, the half-life of dystrophin protein and mRNA is extremely long and therefore relatively smaller dosage of AO gives more sustained exon skipping.<sup>42</sup> However, in myostatin skipping, it is perhaps likely that more frequent redosing is required, to have a more sustained presence of AOs. This may explain the transient and weak effect in terms of whole body weight change we observed *in vivo*. Interestingly, only soleus muscle showed a significant increase in weight and CSA fiber distribution. This is in compliance with some previously published data showing that soleus is the most affected muscle following a systemic approach to knockdown myostatin.<sup>4</sup> Our results represent a proof-of-principle that myostatin knockdown can be obtained by skipping an exon from the transcript by using AOs. Different delivery routes, dosing regimens, and/or AO sequences have to be investigated in future studies to ensure effective *in vivo* knockdown of myostatin expression for maximal therapeutic benefit. This work has the potential to be developed into an efficient treatment for a number of age-related muscle disorders and various neuromuscular disorders, including muscular dystrophies.

## MATERIALS AND METHODS

### Bioinformatics analysis of the myostatin gene to design AOs reagents.

Three different bioinformatics algorithms namely ESE Finder, PESX, and Rescue ESE were used to design antisense reagents. Results from the three algorithms were merged to define ESE sites and used to identify the regions of the myostatin exon 2, which are expected to be optimal targets for exon skipping antisense reagents. A set of 12 antisense reagents of 2'O-methyl RNA (2'OMePS) chemistry were designed to target four different ESE-rich regions of exon 2 of myostatin (Figure 1a).

**AO reagents.** The 12 2'OMePS oligomers tested were obtained from Eurogentec (SA, Seraing, Belgium). The sequences of the 2'OMePS are available on request. PMOs were designed based on the 2'OMePS

sequences. A total of four PMOs were tested and were obtained from Gene Tools (Philomath, OR). PMO sequences are available on request. PMOs conjugated to octa-guanidine dendrimers (so-called Vivo-PMOs) were purchased from Gene Tools.

### Cell culture and transfection of C2C12 cells with the designed antisense reagents.

C2C12 mouse myoblasts were maintained in Dulbecco's modified Eagle's medium (Sigma-Aldrich, Poole, UK) containing 10% fetal calf serum (Sigma-Aldrich), 4 mmol/l L-glutamine, 100 U/ml penicillin and 100 µg/ml streptomycin at 37°C and 8% CO<sub>2</sub>. Cells were split every 24 hours to prevent differentiation. Cells were detached by incubating them with 0.15% trypsin-phosphate-buffered saline for 1 minute at 37°C, and seeded at a density of 1.5 × 10<sup>5</sup> cells/well of a 6-well plate. The antisense reagents of 2'OMePS chemistry were transfected at 250 nmol/l into C2C12 cells using Lipofectamine 2000 (Invitrogen, Paisley, UK). Controls contained Lipofectamine 2000 but no antisense reagent. PMOs were leashed to complementary stretches of negatively charged DNA (obtained from MWG, Ebersberg, Germany) (sequences available on request) for efficient *in vitro* delivery,<sup>24</sup> using Lipofectamine 2000 as transfection reagent. All transfections were performed in Dulbecco's modified Eagle's medium containing 2 mmol/l glutamine (without serum and antibiotics) and after 3–4 hours of transfection, the medium was replaced with full growth medium containing serum as well as antibiotics. The transfections were performed in duplicate and the experiment repeated twice.

**RT-PCR analysis of myostatin exon skipping.** For *in vitro* experiments, 24 hours after transfection, RNA was extracted from each well using QIAshredder/RNeasy extraction kit (Qiagen, Crawley, UK). For *in vivo* experiments, RNA was extracted from blocks using TRIzol reagent (Invitrogen, Scotland, UK). One microgram of RNA was reverse transcribed and resulting complementary DNA amplified using specific primers obtained from MWG, using the Genescript kit (Genesys, Camberley, UK). One micro liter of PCR products obtained was used as a template for nested PCR. Sequences of the primers and details of the PCR protocols used are available on request. The products from nested PCR were separated on 1.2% agarose gel in Tris-borate/EDTA buffer and Hyper Ladder IV (Biolone, London, UK) was used as the marker. Densitometric analysis of the agarose gels was carried out using Gene Tools 3.05 (Syngene, Cambridge, UK) and percentage skipping expressed as amount of skipped product seen relative to total PCR products detected.

**In vitro cell proliferation assay.** A proliferation assay using Cell Titer 96 Aqueous One Solution Cell Proliferation assay (Promega, Madison, WI) was performed, as reported by Cory *et al.*,<sup>43</sup> on cells transfected with different 2'OMePS. Briefly, 24 hours after seeding, the growth media was replaced with serum-free media and cells incubated at 37°C. After 24 hours of subjecting cells to serum-free media, 15 µl of assay reagent was added to 75 µl cells in a 96-well plate. Plates were read at 490 nm. Statistical analysis on the data from the proliferation assay was performed using the individual *t*-test.

**Treatment of mice with PMOs and Vivo-PMOs.** For all the *in vivo* experiments, animals (MF1 or C57Bl10) were bought from Harlan (Blacktown, UK) and in-house maintained, and *in vivo* experimentation conducted under statutory Home Office recommendation, regulatory, ethical and licensing procedures and under the Animals (Scientific Procedures) Act 1986 (project licence PPL 70/7008). For intramuscular delivery, mice were anaesthetized and injected with 3 nmol of 2'OMePS (in 25 µl normal saline) into each of the TA muscles. Control animals were injected with normal saline. Whole body weights were measured weekly. TAs of treated and control mice were excised postmortem after 2 weeks (*n* = 4) and 4 weeks (*n* = 4). Weights were measured and the muscles frozen in iso-pentane cooled with liquid nitrogen. For the systemic administration, C57Bl10 mice were injected intravenously with 6 mg/kg of Vivo-PMO-D

## Myostatin Exon Skipping Leads to Muscle Hypertrophy

(Gene Tools) diluted in 200 µl of normal saline, every week for 5 weeks. Weights were measured weekly and various muscles from treated and control mice were harvested 10 days after the last injection. Cryosectioning was performed at 10 levels through the muscle.

**Immunocytochemistry and morphometry.** Hematoxylin and eosin staining was used to estimate the muscles size. For the estimation of fiber size and distribution, laminin staining was performed. Laminin antibody from Sigma-Aldrich (Dorset, UK) was used as primary antibody, with biotinylated anti-rabbit immunoglobulin G (Dako, Glostrup, Denmark) as secondary antibody. Finally sections were stained with DAB (Vector Laboratories, Burlingame, CA) and slides mounted in DPX (VWR International, Poole, England) after appropriate washings. Immunostaining was also carried out with Dystrophin antibody. For this, H12 Polyclonal Rabbit antibody was used as primary antibody, and Alexa fluor goat anti-rabbit 568 (fluorescein isothiocyanate) (Invitrogen, Paisley, OR) was used as secondary antibody. Slides were mounted in Vectashield mounting medium with DAPI (Vector Laboratories) after appropriate washings with phosphate-buffered saline-Tween. CSA of muscle fibers was measured using SigmaScan Pro 5.0.0 (Systat Software, London, UK).

## ACKNOWLEDGMENTS

This research work was supported by funds from the Muscular Dystrophy Campaign, UK, the Association Française contre les Myopathies (AFM) and the EU Clinigene Network of Excellence (LSHB-CT-2006-018933). We also acknowledge the academic support of the MDEX Consortium (<http://www.mdex.org.uk/>) and the EU TREAT-NMD Network of Excellence (LSHM-CT-2006-036825).

## REFERENCES

- McPherron, AC, Lawler, AM and Lee, SJ (1997). Regulation of skeletal muscle mass in mice by a new TGF- $\beta$  superfamily member. *Nature* **387**: 83–90.
- Schuelke, M, Wagner, KR, Stolz, LE, Hübner, C, Riebel, T, Kömen, W *et al.* (2004). Myostatin mutation associated with gross muscle hypertrophy in a child. *N Engl J Med* **350**: 2682–2688.
- Bogdanovich, S, Perkins, KJ, Krag, TO, Whittemore, LA and Khurana, TS (2005). Myostatin propeptide-mediated amelioration of dystrophic pathophysiology. *FASEB J* **19**: 543–549.
- Foster, K, Graham, IR, Otto, A, Foster, H, Trollet, C, Yaworsky, PJ *et al.* (2009). Adeno-associated virus-8-mediated intravenous transfer of myostatin propeptide leads to systemic functional improvements of slow but not fast muscle. *Regeneration Res* **12**: 85–94.
- Qiao, C, Li, J, Jiang, J, Zhu, X, Wang, B, Li, J *et al.* (2008). Myostatin propeptide gene delivery by adeno-associated virus serotype 8 vectors enhances muscle growth and ameliorates dystrophic phenotypes in mdx mice. *Hum Gene Ther* **19**: 241–254.
- Foster, KW (2009). Eye evolution: two eyes can be better than one. *Curr Biol* **19**: R208–R210.
- Haidet, AM, Rizo, L, Handy, C, Umapathi, P, Eagle, A, Shilling, C *et al.* (2008). Long-term enhancement of skeletal muscle mass and strength by single gene administration of myostatin inhibitors. *Proc Natl Acad Sci USA* **105**: 4318–4322.
- Wagner, KR, Fleckenstein, JL, Amato, AA, Barohn, RJ, Bushby, K, Escolar, DM *et al.* (2008). A phase I/II trial of MYO-029 in adult subjects with muscular dystrophy. *Ann Neurol* **63**: 561–571.
- Whittemore, LA, Song, K, Li, X, Aghajanian, J, Davies, M, Girgenrath, S *et al.* (2003). Inhibition of myostatin in adult mice increases skeletal muscle mass and strength. *Biochem Biophys Res Commun* **300**: 965–971.
- Yang, Z, Zhang, J, Cong, H, Huang, Z, Sun, L, Liu, C *et al.* (2008). A retrovirus-based system to stably silence GDF-8 expression and enhance myogenic differentiation in human rhabdomyosarcoma cells. *J Gene Med* **10**: 825–833.
- Dumonceaux, J, Marie, S, Beley, C, Trollet, C, Vignaud, A, Ferry, A *et al.* (2010). Combination of myostatin pathway interference and dystrophin rescue enhances tetanic and specific force in dystrophic mdx mice. *Mol Ther* **18**: 881–887.
- Weinstein, S and Peer, D (2010). RNAi nanomedicines: challenges and opportunities within the immune system. *Nanotechnology* **21**: 232001.
- Hausen, P and Stein, H (1970). Ribonuclease H. An enzyme degrading the RNA moiety of DNA-RNA hybrids. *Eur J Biochem* **14**: 278–283.
- Zamecnik, PC and Stephenson, ML (1978). Inhibition of Rous sarcoma virus replication and cell transformation by a specific oligodeoxynucleotide. *Proc Natl Acad Sci USA* **75**: 280–284.
- Dominski, Z and Kole, R (1993). Restoration of correct splicing in thalassemic pre-mRNA by antisense oligonucleotides. *Proc Natl Acad Sci USA* **90**: 8673–8677.
- Friedman, KJ, Kole, J, Cohn, JA, Knowles, MR, Silverman, LM and Kole, R (1999). Correction of aberrant splicing of the cystic fibrosis transmembrane conductance regulator (CFTR) gene by antisense oligonucleotides. *J Biol Chem* **274**: 36193–36199.
- Sierakowska, H, Sambade, MJ, Agrawal, S and Kole, R (1996). Repair of thalassemic human  $\beta$ -globin mRNA in mammalian cells by antisense oligonucleotides. *Proc Natl Acad Sci USA* **93**: 12840–12844.
- Dunckley, MG, Manoharan, M, Villiet, P, Eperon, IC and Dickson, G (1998). Modification of splicing in the dystrophin gene in cultured Mdx muscle cells by antisense oligoribonucleotides. *Hum Mol Genet* **7**: 1083–1090.
- Cartegni, L, Chew, SL and Krainer, AR (2002). Listening to silence and understanding nonsense: exonic mutations that affect splicing. *Nat Rev Genet* **3**: 285–298.
- Kinali, M, Arechavala-Gomez, V, Feng, L, Cirak, S, Hunt, D, Adkin, C *et al.* (2009). Local restoration of dystrophin expression with the morpholino oligomer AVI-4658 in Duchenne muscular dystrophy: a single-blind, placebo-controlled, dose-escalation, proof-of-concept study. *Lancet Neurol* **8**: 918–928.
- van Deutekom, JC, Janson, AA, Girjaar, IB, Frankhuizen, WS, Aartsma-Rus, A, Bremmer-Bout, M *et al.* (2007). Local dystrophin restoration with antisense oligonucleotide PRO051. *N Engl J Med* **357**: 2677–2686.
- Hudziak, RM, Barofsky, E, Barofsky, DF, Weller, DL, Huang, SB and Weller, DD (1996). Resistance of morpholino phosphorodiamidate oligomers to enzymatic degradation. *Antisense Nucleic Acid Drug Dev* **6**: 267–272.
- Popplewell, LJ, Trollet, C, Dickson, G and Graham, IR (2009). Design of phosphorodiamidate morpholino oligomers (PMOs) for the induction of exon skipping of the human DMD gene. *Mol Ther* **17**: 554–561.
- Gebski, BL, Errington, SJ, Johnsen, RD, Fletcher, S and Wilton, SD (2005). Terminal antisense oligonucleotide modifications can enhance induced exon skipping. *Neuromuscul Disord* **15**: 622–629.
- Wu, B, Li, Y, Morcos, PA, Doran, TJ, Lu, P and Lu, QL (2009). Octa-guanidine morpholino restores dystrophin expression in cardiac and skeletal muscles and ameliorates pathology in dystrophic mdx mice. *Mol Ther* **17**: 864–871.
- Cartegni, L, Wang, J, Zhu, Z, Zhang, MQ and Krainer, AR (2003). ESEfinder: A web resource to identify exonic splicing enhancers. *Nucleic Acids Res* **31**: 3568–3571.
- Smith, PJ, Zhang, C, Wang, J, Chew, SL, Zhang, MQ and Krainer, AR (2006). An increased specificity score matrix for the prediction of SF2/ASF-specific exonic splicing enhancers. *Hum Mol Genet* **15**: 2490–2508.
- Zhang, XH and Chasin, LA (2004). Computational definition of sequence motifs governing constitutive exon splicing. *Genes Dev* **18**: 1241–1250.
- Zhang, XH, Leslie, CS and Chasin, LA (2005). Computational searches for splicing signals. *Methods* **37**: 292–305.
- Fairbrother, WG, Yeh, RF, Sharp, PA and Burge, CB (2002). Predictive identification of exonic splicing enhancers in human genes. *Science* **297**: 1007–1013.
- Spitali, P, Heemskerck, H, Vossen, RH, Ferlini, A, den Dunnen, JT, 't Hoen, PA *et al.* (2010). Accurate quantification of dystrophin mRNA and exon skipping levels in Duchenne Muscular Dystrophy. *Lab Invest* **90**: 1396–1402.
- Alter, J, Lou, F, Rabinowitz, A, Yin, H, Rosenfeld, J, Wilton, SD *et al.* (2006). Systemic delivery of morpholino oligonucleotide restores dystrophin expression bodywide and improves dystrophic pathology. *Nat Med* **12**: 175–177.
- Popplewell, LJ, Adkin, C, Arechavala-Gomez, V, Aartsma-Rus, A, de Winter, CL, Wilton, SD *et al.* (2010). Comparative analysis of antisense oligonucleotide sequences targeting exon 53 of the human DMD gene: Implications for future clinical trials. *Neuromuscul Disord* **20**: 102–110.
- Gebski, BL, Mann, CJ, Fletcher, S and Wilton, SD (2003). Morpholino antisense oligonucleotide induced dystrophin exon 23 skipping in mdx mouse muscle. *Hum Mol Genet* **12**: 1801–1811.
- Carnac, G, Ricaud, S, Vernus, B and Bonniere, A (2006). Myostatin: biology and clinical relevance. *Mini Rev Med Chem* **6**: 765–770.
- Patel, K and Amthor, H (2005). The function of Myostatin and strategies of Myostatin blockade-new hope for therapies aimed at promoting growth of skeletal muscle. *Neuromuscul Disord* **15**: 117–126.
- Amantana, A and Iversen, PL (2005). Pharmacokinetics and biodistribution of phosphorodiamidate morpholino antisense oligomers. *Curr Opin Pharmacol* **5**: 550–555.
- Arora, V, Devi, GR and Iversen, PL (2004). Neutrally charged phosphorodiamidate morpholino antisense oligomers: uptake, efficacy and pharmacokinetics. *Curr Pharm Biotechnol* **5**: 431–439.
- Langleby, B, Thomas, M, Bishop, A, Sharma, M, Gilmour, S and Kambadur, R (2002). Myostatin inhibits myoblast differentiation by down-regulating MyoD expression. *J Biol Chem* **277**: 49831–49840.
- Iversen, PL (2001). Phosphorodiamidate morpholino oligomers: favorable properties for sequence-specific gene inactivation. *Curr Opin Mol Ther* **3**: 235–238.
- Morcos, PA, Li, Y and Jiang, S (2008). Vivo-Morpholinos: a non-peptide transporter delivers Morpholinos into a wide array of mouse tissues. *BioTechniques* **45**: 613–4, 616, 618 passim.
- Ghahramani Seno, MM, Graham, IR, Athanasopoulos, T, Trollet, C, Pohlschmidt, M, Chromton, MR *et al.* (2008). RNAi-mediated knockdown of dystrophin expression in adult mice does not lead to overt muscular dystrophy pathology. *Hum Mol Genet* **17**: 2622–2632.
- Cory, AH, Owen, TC, Bartrop, JA and Cory, JG (1991). Use of an aqueous soluble tetrazolium/formazan assay for cell growth assays in culture. *Cancer Commun* **3**: 207–212.